0026-895X/92/020265-08$03.00/0

MOLECULAR PHARMACOLOGY, 42:265-272

Cloned Mouse *N*-Acetyltransferases: Enzymatic Properties of Expressed *Nat-1* and *Nat-2* Gene Products

KAREN J. MARTELL, GERALD N. LEVY, and WENDELL W. WEBER

Department of Pharmacology, The University of Michigan Medical School, Ann Arbor, Michigan 48109-0626

Received December 13, 1991; Accepted May 8, 1992

SUMMARY

N-Acetylation plays an important role in the metabolism of a wide variety of hydrazine drugs and arylamine drugs and carcinogens. Humans have genetically determined differences in their *N*-acetyltransferase activities and are phenotypically classified as rapid or slow acetylators. Mice have a similar genetic polymorphism in *N*-acetyltransferase activity and have been used as models of the human polymorphism in many studies of the toxicology and carcinogenicity of arylamines. Recently, two *N*-acetyltransferase genes, *Nat-1* and *Nat-2*, were cloned from rapid (C57BL/6J) and slow (A/J) acetylator mouse strains. The genomic clone encoding NAT-1 is identical in rapid and slow acetylator mouse strains, whereas the clone encoding NAT-2 differs between rapid and slow strains by a single base pair, which changes the encoded amino acid from Asn^{99} in the rapid acetylator strain to Ile^{99} in the slow acetylator strain. In this report, the *N*-acetylation polymorphism in mice was investigated by transiently expressing the cloned *N*-acetyltransferase genes in COS-1 cells. The intronless coding regions of *Nat-1* and *Nat-2* showed different substrate specificities; isoniazid was a preferred substrate for NAT-1, whereas *p*-aminobenzoic acid was preferred for $NAT\text{-}2^{99asn}$ and $NAT\text{-}2^{99ile}$. All three enzymes acetylated 2-aminofluorene, but none of them acetylated sulfamethazine. Kinetic constants determined for the expressed enzymes with 2-aminofluorene and *p*-aminobenzoic acid indicated that K_m values were not significantly different between the enzymes, although the V_{max} value of $NAT\text{-}2^{99asn}$ was consistently 2-3-fold higher than that of NAT-1 or $NAT\text{-}2^{99ile}$. *Nat-1* and *Nat-2* encoded mRNAs of approximately 1.4 kilobases in livers of rapid and slow acetylators. Nat-2 mRNA was more abundant in liver than Nat-1 mRNA. The abundance of Nat-2 mRNA and Nat-1 mRNA was equivalent in both rapid and slow acetylator mouse strain livers. Incubation of transfected COS-1 cell cytosols at 37° showed that the time for decline of NAT activity to 50% of its initial value was 45 hr for NAT-1, 60 hr for $NAT\text{-}2^{99asn}$, and 4 hr for $NAT\text{-}2^{99ile}$. This 15-fold difference in the heat stability of the rapid and slow isoforms of NAT activity was also observed in cytosols from rapid and slow acetylator livers. Comparison of the rates of translation of the rapid and slow isoforms of NAT-2 in an *in vitro* system showed that $NAT\text{-}2^{99asn}$ was translated at approximately twice the rate of $NAT\text{-}2^{99ile}$. These data indicate that *Nat-1* and *Nat-2* gene sequences encode functionally distinct NAT activities, which are transcribed in livers of rapid and slow acetylators. In addition, there are differences in heat stability and in the rates of translation of the rapid and slow isoforms NAT-2, which may contribute to the phenotypic differences observed in the genetically rapid and slow acetylator mice.

The *N*-acetylation polymorphism is an inherited variation in drug biotransformation that occurs in humans, animals, and bacteria and is one of the oldest known pharmacogenetic traits. NAT catalyzes the transfer of an acetyl group from AcCoA to the free amine moiety of an arylamine or to an hydrazine, by a ping-pong BiBi kinetic reaction mechanism (1). Hydrazine drugs and arylamine drugs and carcinogens are among the best known substrates for NAT, and several of these compounds have also been linked to idiosyncratic drug reactions and to chemical carcinogenesis in "rapid" or "slow" acetylators (reviewed in Ref. 2). The relationship between acetylator status and drug therapy or carcinogenesis has been studied in several animal species, including rabbits, hamsters, rats, and mice (3-7).

Recently, several reports have identified the molecular basis of rapid and slow acetylation in humans, rabbits, hamsters, and mice (8-18). In all of these species, at least two *NAT* genes, designated *Nat-1* and *Nat-2*, have been identified. The cloned human *NAT1* and *NAT2* gene products have different sub-

This work was partially supported by United States Public Health Service Grants GM 44965, 5T32 GM 07544, OH 00081, and CA 39018.

ABBREVIATIONS: NAT, generic term for acetyl coenzyme A:arylamine *N*-acetyltransferase protein or activity from any species; *Nat-1*, mouse gene encoding monomorphic *N*-acetyltransferase; *Nat-2*, mouse gene encoding polymorphic *N*-acetyltransferase; $Nat\text{-}2^b$, mouse allelic variant of *Nat-2* cloned from the C57BL/6J strain (rapid acetylator); $Nat\text{-}2^a$, mouse allelic variant of *Nat-2* cloned from the A/J strain (slow acetylator); Nat-1, mRNA transcript of the *Nat-1* gene; Nat-2, mRNA transcript of the *Nat-2* gene; NAT-1, enzyme protein encoded by the *Nat-1* gene; $NAT\text{-}2^{99asn}$, enzyme protein encoded by the $Nat\text{-}2^b$ gene; $NAT\text{-}2^{99ile}$, enzyme protein encoded by the $Nat\text{-}2^a$ gene; A, A/J; B6, C57BL/6J; 2-AF, 2-aminofluorene; 2-AAF, 2-acetylaminofluorene; INH, isoniazid; PABA, *p*-aminobenzoic acid; SMZ, sulfamethazine; BES, *N,N*-bis(2-hydroxyethyl)-2-aminoethanesulfonic acid; SDS, sodium dodecyl sulfate; AcCoA, acetyl-coenzyme A; bp, base pairs; kb, kilobases; SET, 0.5 M NaCl, 0.02 M Tris·Cl (pH 7.8), 1 mM EDTA.

strate specificities and kinetic constants, which are comparable to those of the respective NATs purified from human liver (9). These results are consistent with one of the hypotheses of Jenne *et al.* (19), based upon metabolic clearance studies with INH and *para*-aminosalicilic acid, that two separate NATs, with distinct substrate specificities, are present in human liver. Similarly, transient expression of cloned rabbit *NAT* genes in COS-1 cells revealed that the expressed rabbit NAT enzymes have substrate specificity profiles that are consistent with *in vivo* metabolism (14, 20).

Although the rabbit has been used as a model of the acetylation polymorphism of humans, the molecular basis of slow acetylation differs in these species. In humans, point mutations of the coding region cause several amino acid changes in the slow allelic variants of human *NAT2* (9, 13). The way that these mutations result in the slow phenotype has not been fully examined. Defective translation is suggested to be responsible in the case of the M1 slow allelic variant, whereas the M2 variant produces an enzyme that is 4-fold less stable at 37° than the wild-type enzyme (10). In rabbits, deletion of the *NAT2* gene is the basis of the slow acetylator phenotype (14, 15). Despite the different genetic mechanisms that underlie the slow phenotype in humans and rabbits, slow acetylation in both species appears to be due to the absence or reduction of the polymorphic NAT enzyme. (10, 14–16).

Over the last 15 years, the inbred mouse model of human acetylation polymorphism has been used extensively for biochemical, toxicological, and carcinogenesis experiments (reviewed in Ref. 2). In order to investigate the molecular basis of slow acetylation in the mouse, we have recently isolated genomic clones encoding *Nat-1* and *Nat-2* genes from rapid (B6) and slow (A) inbred mouse strains (18). The *Nat-2* genes obtained from the B6 (*Nat-2*^{b}) and A (*Nat-2*^{a}) mouse strains differ by a single nucleotide change, in which adenine at position 296 in B6 is replaced by thymine in A mice. The nucleotide substitution in the *Nat-2* gene changes the deduced amino acid at position 99 from asparagine in B6 to isoleucine in A mice. The protein products of *Nat-1, Nat-2*^{b}, and *Nat-2*^{a} are designated NAT-1, NAT-2^{99asn}, and NAT-2^{99ile}, respectively. The amino acid change in NAT-2 alters the character of the surrounding peptide fragment from hydrophilic in NAT-2^{99asn} to hydrophobic in NAT-2^{99ile}, and this difference may contribute to the differences seen in rapid and slow acetylation in the *N*-acetylation polymorphism of the mouse.

In the present study, we demonstrate that the intronless coding regions of *Nat-1* and *Nat-2* encode NAT enzymes with distinct substrate specificities. Northern blot analysis indicates that the mRNAs of both genes are expressed in mouse liver. Finally, this report is the first to demonstrate a correlation between the *in vitro* heat stability of cloned NAT enzymes and that of hepatic cytosol. The heat stability data and our efficiency of translation data indicate that the NAT-2^{99asn} and the NAT-2^{99ile} differ in such a way as to reflect the phenotypic differences found in the respective strains from which they were cloned.

Materials and Methods

Animals. Inbred B6 and A mice were purchased from The Jackson Laboratory (Bar Harbor, ME). Mice were housed 2–6/standard shoebox cage and were maintained at 25°, on a 12-hr light/dark cycle. Animals were given water and Purina Mouse Chow 9F 5020 *ad libitum*. Mature mice of both sexes were used.

Materials. Restriction endonucleases and other DNA-modifying enzymes were purchased from BRL (Bethesda, MD) and New England Biolabs (Beverly, MA). *Bam*HI linkers were from New England Biolabs. Chemicals and buffers were molecular biology grade and obtained from Sigma (St. Louis, MO) or IBI (New Haven, CT). All cell culture media were obtained from GIBCO BRL. The RNA molecular weight marker II was from Boehringer Mannheim Biochemicals (Indianapolis, IN). Hybond N and [α-^{32}P]UTP (800 Ci/mmol) were purchased from Amersham (Arlington Heights, IL). pGEM 7Zf(−), RNAgents total RNA isolation kit, PolyATract mRNA isolation system, and the Riboprobe II Core system were purchased from Promega (Madison, WI). A Sequenase version II kit was purchased from United States Biochemicals (Cleveland, OH). A Geneclean kit was obtained from Bio 101 (La Jolla, CA). Data were plotted with GRAPHpad INPLOT version 3.1 (San Diego, CA). Kinetic constants were calculated using the Cleland Hyper program (obtained from Dr. R. Viola, University of Akron, Akron, OH).

Plasmid construction. The intronless coding regions and adjacent segments of the 5′ and 3′ noncoding regions of *Nat-1* and *Nat-2* from the B6 mouse were subcloned into pGEM 7Zf(−), to serve as templates for riboprobe production and to facilitate subsequent subcloning into mammalian expression vectors. pB6Nat-5HE, which contained *Nat-1* (18), was digested with *Acc*I (bp −104) and *Ssp*I (bp 1118), to yield a fragment of 1.222-kb. pB6Nat-5H, which contained *Nat-2* (18), was digested with *Alu*I (bp −124 and 1003), to yield a fragment of 1.127 kb. Numbers in parentheses indicate the restriction sites in the genes, according to the published sequence (18). The *Nat-1* fragment was end-filled with Klenow, whereas the *Alu*I digest of *Nat-2* produced blunt-ended fragments. The blunted fragments were ligated to *Bam*HI linkers, digested with *Bam*HI, and subcloned into the *Bam*HI site of pGEM 7Zf(−). The recombinant plasmids were mapped to confirm orientation, and the resulting constructs were referred to as pN1B6T, which has the 1.222-kb fragment containing the coding region of *Nat-1*, and pN2B6T, which has the 1.127-kb fragment containing the coding region of *Nat-2*^{b}.

The coding region of *Nat-2*^{a} from the slow acetylator A strain was subcloned into pGEM 7Zf(−), to make the recombinant plasmid pN2AJT, as follows. *Nat-2*^{a}, obtained by polymerase chain reaction amplification (18), was digested with *Bsu*36I (bp 205 and 645), to release a 450-bp fragment surrounding the point mutation (bp 296) found between *Nat-2*^{b} and *Nat-2*^{a}. The 450-bp *Bsu*36I fragment was isolated from agarose gel using Geneclean and was subcloned into *Bsu*36I-digested pN2B6T. Recombinant plasmids were mapped with *Bst*XI to confirm orientation and then sequenced to ascertain that the insert was free of *Taq* polymerase error. The resulting plasmid, pN2AJT, is identical to pN2B6T, except for the base change at position 296, where a T is present in pN2AJT instead of an A in pN2B6T.

Transient expression in COS-1 cells. pN1B6T, pN2B6T, and pN2AJT were digested with *Bam*HI, to release the coding regions of *Nat-1, Nat-2*^{b}, and *Nat-2*^{a}, respectively. All inserts were purified from the agarose gel with Geneclean and subsequently ligated into *Bgl*II-digested pCMV-Neo, a mammalian expression vector that was a gift from Dr. Michael Uhler, Department of Biological Chemistry, University of Michigan. pCMV-Neo contains an SV40 origin of replication and utilizes the strong human cytomegalovirus promoter to drive expression of the cloned insert (21). Recombinant plasmids were mapped to ensure that they had the correct orientation, and the resulting constructs were designated as follows: pCMVN1, which encodes the monomorphic NAT-1 enzyme; pCMVN2B6, which encodes NAT-2^{99asn}; and pCMVN2AJ, which encodes NAT-2^{99ile}. COS-1 cells were acutely transfected using a calcium phosphate precipitation technique (22). Subconfluent cells (approximately 750,000 cells on a 10-cm culture dish) were co-transfected with 16 μg of the appropriate NAT-encoding plasmid and 4 μg of pCMV-βGal (a *lacZ*-encoding expression construct), in 1 ml of 1× BES-buffered saline (25 mM BES, 140 mM

NaCl 1 mM Na_2HPO_4 [pH G.95]) containing 250 mM $CaCl_2$. Cells were harvested 2 days after transfection and were sonicated in 400 μl of lysing buffer (20 mM Tris·HCl, pH 7.8, 1 mM EDTA, 1 mM dithiothreitol, 50 μM phenylmethylsulfonyl fluoride, 10 μM leupeptin), to disrupt cell membranes. Homogenates were centrifuged at 4° at 14,000 rpm, in an Eppendorf microfuge. The supernatant fractions were diluted so that no more than one third of the substrate would become acetylated and were assayed for NAT activity as described below.

To compare expressed enzymes with NAT activities found in liver, 20% homogenates of livers from B6 and A mice were prepared in lysing buffer. The cytosolic fraction was prepared by centrifugation of the homogenate at 100,000 × *g* for 1 hr. The cytosols were diluted and then assayed for NAT activity and protein content as described below.

Assay of NAT activity. NAT activity for 2-AF, PABA, SMZ, and INH was determined using an assay described previously (23), except that for 2-AF the reaction was stopped with 100 μl of acetonitrile instead of 50 μl of 20% trichloroacetic acid. Other modifications were used for the INH assay, as described below. The amounts of acetylated product and nonacetylated substrate for 2-AF, PABA, and SMZ were determined by a high performance liquid chromatography procedure modified from that of Kawakubo *et al.* (24). An aliquot of the supernatant from the NAT assay was injected onto a reverse phase C-18 column (Varian MCH-NCAP-5, 4 mm × 15 cm) and eluted at a flow rate of 1.2 ml/min. For 2-AF/2-AAF the solvent system was 20 mM potassium phosphate, pH 4.5/CH_3CN (57:43), with detection at 280 nm. The retention times were 6.3 min for 2-AAF and 8.0 min for 2-AF. For PABA/*N*-acetyl-PABA the solvent system was 50 mM acetic acid/CH_3CN (90:10), with detection at 266 nm. The retention times were 3 min for PABA and 7 min for *N*-acetyl-PABA. For SMZ/*N*-acetyl-SMZ the solvent system was 50 mM acetic acid/CH_3CN (90:10), with detection at 260 nm. The retention times were 7 min for SMZ and 10 min for *N*-acetyl-SMZ. All compounds were quantitated by comparison of the integrated area of the elution peak with that of known amounts of standards. NAT activities were normalized to the amount of protein, as determined by a Bradford assay kit using a bovine serum albumin standard (Bio-Rad, Richmond, CA). All NAT activities were normalized to β-galactosidase activity, to control for differences in transfection efficiency between individual culture dishes (25, 26). β-Galactosidase activity was determined by previously reported procedures (21, 27). Kinetic constants (apparent K_m and V_{max}) were calculated with the Cleland Hyper program (28). Enzyme stability experiments were carried out by incubating appropriately diluted cytosol at 37° for the specified periods of time and then removing samples from the tubes for enzyme assays.

INH-acetylating activity of the expressed NATs was assayed using the recycling system described above, except that the acetylation reaction was terminated by the addition of 30 μl of 20% trichloroacetic acid. To determine the amount of acetylated INH formed, 1 ml of 0.8 M potassium borate, pH 9.0, was added and the absorbance at 303 nm was measured. Under these conditions, an increase in absorbance of 6.32 indicates formation of 1 μmol of acetylated product (29).

Northern blot analysis. Total RNA and, subsequently, poly(A)$^+$ RNA were isolated from livers of adult B6 and A/J mice using the procedures outlined in the RNAgents total RNA isolation kit and the PolyATract mRNA isolation system from Promega. For the Northern blot analysis, 8 μg of poly(A)$^+$ RNA per lane were subjected to electrophoresis on a 1% agarose gel containing 6% formaldehyde and were transferred to Hybond N membranes, using standard Northern blotting procedures. Filters were prehybridized at 60° for 2 hr in 0.4 M sodium phosphate buffer (pH 7.0) containing 1 mM EDTA, 5% (w/v) SDS, 1 mg/ml bovine serum albumin, and 50% (v/v) formamide. Filters were hybridized in the same solution at 50° for 18 hr, with riboprobes specific for Nat-1 or Nat-2 mRNA. The specific probes corresponded to the 3′ untranslated regions of Nat-1 and Nat-2, which were 42% identical. SP6 RNA polymerase transcribed a 189-bp antisense riboprobe from pN1B6T linearized with *Nde*I (bp 929) and a 148-bp antisense riboprobe from pN2B6T linearized with *Cla*I (bp 855) (the terminating nucleotide in the coding region was bp 870). The riboprobes were labeled to a specific activity of 7×10^6 cpm/μg, using the Riboprobe II Core system and [α-^{32}P]UTP (800 Ci/mmol). Filters were washed sequentially in 0.5× SET, containing 0.1% (w/v) sodium pyrophosphate, for 5, 10, and 15 min at room temperature and then for 10 min at 55°. The filter hybridized with the Nat-1-specific probe was further washed for 20 min at 60° in 0.5× SET containing 0.1% (w/v) sodium pyrophosphate and then twice for 30 min at 70° in 0.1× SET containing 0.1% (w/v) sodium pyrophosphate, to remove background hybridization. The stringent washes did not appreciably diminish the hybridization signal to the Nat-1 message. Blots were exposed at room temperature, for 2 hr in the case of Nat-2 and for 6 hr in the case of Nat-1, to Kodak X-OMAT film overlaid with intensifying screens.

The blots were stripped of the Nat-1 or Nat-2 riboprobes by boiling for 10 min in distilled H_2O. Complete removal of the riboprobe was confirmed by the absence of any signal on an autoradiogram exposed to the stripped filters overnight. The blots were then hybridized to a riboprobe corresponding to the coding region of mouse γ-actin. The plasmid encoding mouse γ-actin, pGEMblue-γ-actin, was a gift of Dr. Michael Uhler, Department of Biological Chemistry, University of Michigan. The plasmid was linearized with *Eco*RI, so that a 1.2-kb riboprobe could be synthesized by the procedure outlined above. The blot was prehybridized, hybridized, washed, and exposed as described above for the Nat-2-specific riboprobe. The radioactivity on the blots hybridized to the NAT riboprobes was measured for 50 min with a Betascope model 603 blot analyzer (Betagen Corporation, Waltham, MA).

***In vitro* translation assays.** *In vitro* translation of *Nat-1* and *Nat-2* gene products was performed with the TNT coupled reticulocyte lysate transcription/translation system from Promega. Reactions containing 1 μg of supercoiled plasmid DNA and T7 RNA polymerase were set up according to the manufacturer's instructions. Briefly, plasmids containing the protein-coding regions of either *Nat-1*, *Nat-2*^{b}, or *Nat-2*^{a} cloned downstream from a T7 RNA polymerase promoter (pN1B6T, pN2B6T, and pN2AJT, respectively; see Plasmid construction above) were incubated in a 50-μl reaction volume with 40 μCi of [^{35}S]methionine (1000 Ci/mmol; Amersham) at 30°, for up to 120 min. Ten-microliter aliquots were removed at 15, 30, 60, and 120 min, and the reaction was stopped by the addition of SDS loading buffer, on ice. The samples and 4 μl of ^{14}C-methylated molecular weight markers (Amersham) were denatured by heating to 80° for 5 min and were then loaded onto denaturing 10% SDS-polyacrylamide gels. The gels were run for 1.5 hr at 30 mA, after which they were washed in water for 1 hr to remove unincorporated [^{35}S]methionine, fixed for 20 min in a 15:65:20 solution of acetic acid/isopropanol/water, and soaked for 20 min in scintillant (Amplify; Amersham). Gels were dried under vacuum at 80° for 3 hr and then overnight without heat and were exposed to X-ray film (HyperFilm; Amersham), with intensifying screens, for 8 hr. Radioactivity of each band was counted overnight using a Betascope model 603 blot analyzer, as described above for the Northern blot analysis.

Results

Substrate specificity of expressed NATs. Substrate preferences were determined by NAT activity assay of cytosols from COS-1 cells transiently transfected with expression constructs of the intronless coding regions of *Nat-1*, *Nat-2*^{b}, and *Nat-2*^{a}. Fig. 1 illustrates the results of substrate specificity determinations with 2-AF, PABA, SMZ, and INH. Mock-transfected COS-1 cells had no NAT activity with these substrates (data not shown). All expressed NATs metabolized 2-AF, although NAT-2^{99asn} had the highest acetylating activity. NAT-1 and NAT-2^{99ile} had comparable levels of activity for 2-AF, which were about half the activity of NAT-2^{99asn}. PABA was not acetylated by NAT-1 but was a substrate for both

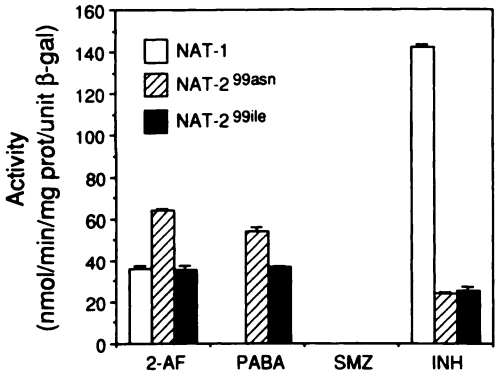

Fig. 1. Substrate specificity of arylamine NATs expressed in COS-1 cells. Cytosols from acutely transfected COS-1 cells were assayed for NAT activity with 0.1 mM 2-AF, PABA, or SMZ and 0.1 mM AcCoA, as described in Materials and Methods. For the INH assay, 11 mM INH and 2 mM AcCoA were used in the assay described in Materials and Methods. Cytosols were obtained from cells transfected with expression vectors encoding the monomorphic NAT-1 enzyme, NAT-2^{99asn}, and NAT-2^{99ile}. Values are presented as the average ± standard error for three experiments.

TABLE 1

Kinetic constants for 2-AF

Values presented are averages ± standard errors (three experiments). Kinetic constants were compared with those determined for NAT-2^{99asn} by the unpaired *t* test.

Enzyme	AcCoA	Apparent K_m	V_{max}
	mM	μM	nmol/min/mg of protein/unit of β-galactosidase
NAT-1	0.1	22.4 ± 4.1[a]	35.9 ± 4.6[b]
NAT-2^{99asn}	0.1	40.1 ± 7.3	153.0 ± 26.3
NAT-2^{99ile}	0.1	26.8 ± 4.5[a]	74.1 ± 17.1[b]
NAT-1	0.5	18.4 ± 7.1[a]	109.0 ± 14.0[b]
NAT-2^{99asn}	0.5	39.5 ± 8.6	276.2 ± 62.4
NAT-2^{99ile}	0.5	21.5 ± 2.8[a]	94.9 ± 9.1[b]

[a] Not significantly different from NAT-2^{99asn} ($p > 0.05$).
[b] Significantly different from NAT-2^{99asn} ($p < 0.05$).

isoforms of NAT-2, with NAT-2^{99asn} showing a higher level of activity than NAT-2^{99ile}. SMZ was not a substrate for any of the NATs. Addition of SMZ to the PABA assay indicated that the enzymes were not inhibited by SMZ (data not shown). INH was acetylated preferentially by NAT-1. NAT-2^{99asn} and NAT-2^{99ile} were also able to metabolize INH, but at a rate one seventh that of NAT-1. Thus, all genes encoded functional NATs, including the slow allelic variant NAT-2^{99ile}.

Kinetic properties of NAT-1, NAT-2^{99asn}, and NAT-2^{99ile}. To explore further the functional differences between the monomorphic and polymorphic forms of mouse NATs, enzyme kinetic constants were determined with 2-AF and PABA. With 2-AF as a substrate (Table 1), the apparent K_m values for the three enzymes did not differ significantly. However, NAT-2^{99asn} had at least a 2-fold higher V_{max} value than did either NAT-1 or NAT-2^{99ile}, at both 0.1 mM and 0.5 mM AcCoA concentrations. It should be noted that differences in transfection efficiency and, hence, protein expression were normalized by assaying for the activity of the co-transfected reporter gene β-galactosidase and not by measuring the amounts of NAT-1 and NAT-2. Therefore, the V_{max} data must be interpreted cautiously.

With PABA as a substrate, the apparent K_m values of NAT-2^{99asn} and NAT-2^{99ile} were not significantly different (Table 2). The V_{max} values for NAT-2^{99asn} were approximately 1.5-fold greater for NAT-2^{99ile} at both AcCoA concentrations. For both

TABLE 2

Kinetic constants for PABA

Values presented are averages ± standard errors (three experiments). Kinetic constants were compared with those determined for NAT-2^{99asn} by the unpaired *t* test. PABA is not a substrate for NAT-1, as shown in Fig. 1 and, therefore, no kinetic constants were determined for this enzyme with this substrate.

Enzyme	AcCoA	K_m	V_{max}
	mM	μM	nmol/min/mg of protein/unit of β-galactosidase
NAT-2^{99asn}	0.1	6.8 ± 1.9	23.5 ± 2.1
NAT-2^{99ile}	0.1	5.3 ± 2.1[a]	14.2 ± 1.8[b]
NAT-2^{99asn}	0.5	23.0 ± 3.1	164.6 ± 7.7
NAT-2^{99ile}	0.5	15.3 ± 2.6[a]	112.3 ± 5.7[c]

[a] Not significantly different from NAT-2^{99asn} ($p > 0.05$).
[b] Significantly different from NAT-2^{99asn} ($p < 0.05$).
[c] Significantly different from NAT-2^{99asn} ($p < 0.01$).

2-AF and PABA, increasing the AcCoA concentration increased the V_{max} values for all three enzymes.

Northern blot analysis of *Nat-1* and *Nat-2*. To determine whether Nat-1 and Nat-2 mRNA were present in rapid and slow acetylator livers, Northern blots of poly(A)$^+$ mRNA from B6 and A mouse livers were probed with ^{32}P-labeled riboprobes designed to hybridize specifically to either Nat-1 or Nat-2 mRNA. The riboprobes corresponded to the nonhomologous (42% identity) 3′ noncoding regions of *Nat-1* or *Nat-2* and, therefore, the probes were specific for the respective messages under the conditions used. The autoradiograms of the Northern blots showed that both Nat-1 and Nat-2 were expressed in liver (Fig. 2) and that Nat-2 was more abundant than Nat-1. Both messages migrate just beyond the 1.6-kb marker, at approximately 1.4 kb. Equivalent amounts of mRNA were loaded onto the gels used for the Northern blots, as demonstrated by the similar abundance of γ-actin mRNA in B6 and A liver (Fig. 2).

Because small differences in relative mRNA abundance on the Northern blot may not be apparent to the eye, the amount of radioactivity associated with each of the riboprobe signals on the Northern blots was quantified by direct counting of the β-emitting isotope. The amount of riboprobe that hybridized to the Nat-1 mRNA (Fig. 3) was similar in slow (area A3 = 4.7 cpm) and rapid (area A4 = 4.7 cpm) acetylator livers, indicating that similar quantities of Nat-1 mRNA are present in rapid and slow acetylator livers. Similarly, the amount of riboprobe that hybridized to the Nat-2 mRNA (Fig. 3) was similar in slow (area A1 = 153.3 cpm) and rapid (area A2 = 150.4 cpm) acetylator livers, which indicates that similar quantities of Nat-2 mRNA are present in rapid and slow acetylator livers. The background radioactivity value of the Northern blot hybridized with the Nat-1 riboprobe (area A5 = 1.6 cpm) was lower than that of the Northern blot hybridized with the Nat-2 riboprobe (area A6 = 4.6 cpm), and this probably reflects the more stringent washing of the Nat-1 blot (described in Materials and Methods).

***In vitro* translation of gene products of *Nat-1* and *Nat-2*.** The *in vitro* coupled transcription/translation system was used to determine the time course of the *in vitro* translation of *Nat-2*^{b}, *Nat-2*^{a}, and *Nat-1* (Fig. 4, A, B, and C, respectively). The rate of translation of *Nat-2*^{a} was about half that of *Nat-2*^{b} in this system (Fig. 4D). The translation of *Nat-1*, performed in the same *in vitro* system, was more rapid and the product was more abundant than either form of *Nat-2* (Fig. 4E). The difference between translation of *Nat-1* and *Nat-2* most likely reflects the difference in vector constructs used in this system.

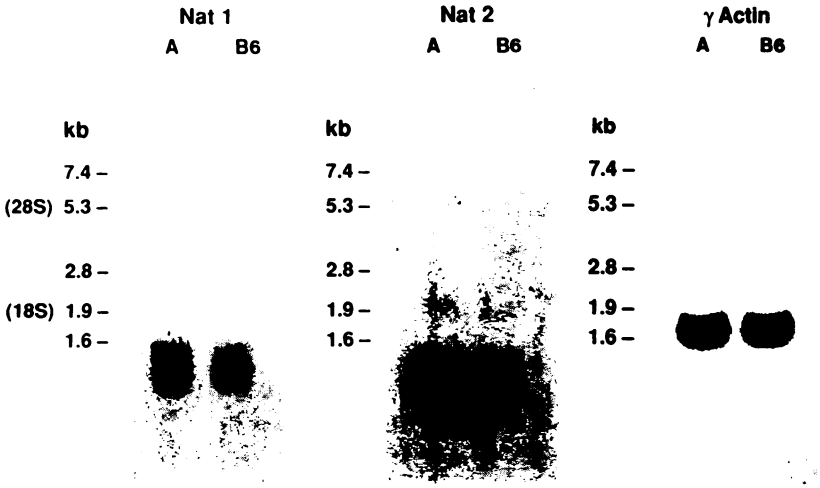

Fig. 2. Northern blot analysis of Nat-1 and Nat-2 mRNA expression in liver. Each sample lane was loaded with 8 μg of poly(A)$^+$ RNA from liver of A or B6 mice, as indicated. Molecular weight markers, to the *left* of each blot, indicate the size in kb and the migration of each subunit of rRNA. The figure shows the autoradiogram of the Northern blot hybridized with Nat-1-, Nat-2-, and γ-actin-specific probes.

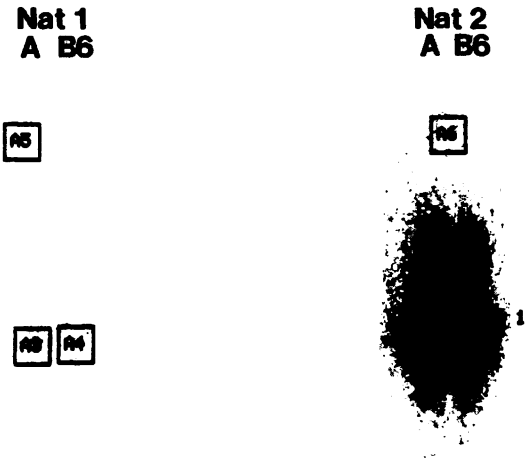

Fig. 3. Betascan counting of radioactivity associated with Nat-1 and Nat-2. The Northern blots shown in Fig. 2 were counted for 50 min with a Betascope blot analyzer, to determine the relative amounts of radiolabeled riboprobe that hybridized to Nat-1 and Nat-2 bands, respectively. Counts associated with the Northern blot hybridized with the Nat-1 riboprobe are as follows: background (*A5*), 1.6 cpm; mRNA from A mice (*A3*), 4.7 cpm; mRNA from B6 mice (*A4*), 4.7 cpm. Counts associated with the Northern blot hybridized with the Nat-2 riboprobe are: background (*A6*), 4.6 cpm; mRNA from A mice (*A1*), 153.3 cpm; mRNA from B6 mice (*A2*), 150.4 cpm.

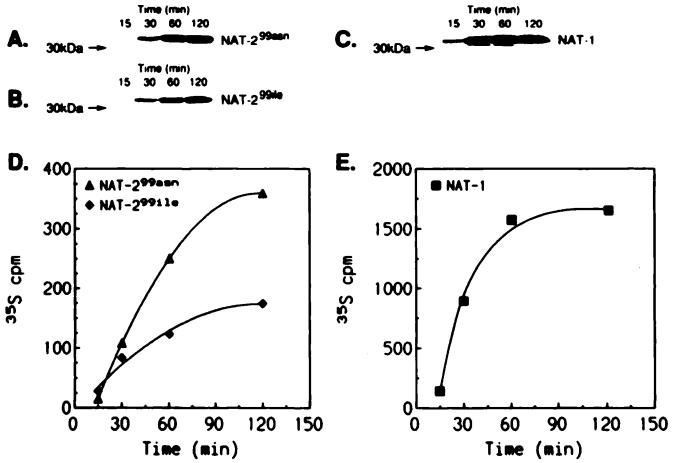

Fig. 4. *In vitro* translation of NAT gene products. A, Autoradiogram of expressed NAT-2^{99asn} protein assayed after 15, 30, 60, and 120 min of *in vitro* coupled transcription/translation, relative to a 30-kDa protein molecular mass marker band. B, Same as A, except expressed NAT-2^{99ile} protein levels. C, Same as A, except expressed NAT-1 protein levels. D, Time course of NAT-2^{99asn} and NAT-2^{99ile} protein expression after quantification by direct counting of the incorporated [^{35}S]methionine in the protein bands described above. E, Same as D, except NAT-1 expression. Counting was performed once for each band, and values were converted to ^{35}S cpm after background subtraction. A second assay using linearized DNA templates produced similar results (data not shown), but the expressed protein levels were 5–10-fold less and, thus, could not be averaged with the present results.

Both *Nat-2^b* and *Nat-2^a* have three upstream ATG sequences that could cause false initiation of the translated product (the encoded proteins terminate before or shortly into the true open reading frame), whereas the *Nat-1* sequence has only one upstream ATG sequence (18).

One ancilliary finding of this experiment is that the molecular mass of all three expressed gene products is approximately 31 kDa. This agrees with the estimate for purified mouse liver NAT (30) and is slightly less than the value of 33.7 kDa calculated based on the deduced amino acid sequence. A control experiment lacking the plasmid template produced no protein bands (data not shown).

Enzyme stability of NAT-1 and NAT-2. Predicted secondary structure of NAT-1, NAT-2^{99asn}, and NAT-2^{99ile} differed greatly in some regions, with regard to α-helix and β-sheet structures (according to predictions made by Chou and Fasman) (31) (data not shown) and hydropathy indices (according to Kyte-Doolittle analysis) (18). Such structural differences could affect functional and stability differences between the three enzymes, as already examined in the substrate specificity and kinetic constant determinations. Stability differences between the enzymes were examined, because this was suggested previously as a possible mechanism of slow acetylation in mice (30) and was shown recently to be the mechanism of slow acetylation in some humans (10).

Transfected COS-1 cell cytosolic fractions were incubated at 37°, to determine the *in vitro* heat stability of expressed NAT-1 and NAT-2. Results are presented (Fig. 5) as the percentage of activity remaining after incubation at 37° for the indicated period of time. The initial activity values for acetylation of 2-AF (in nmol/min/mg of protein/unit of β-galactosidase), determined at time zero, were as follows: NAT-1, 27.1; NAT-2^{99asn}, 82.4; and NAT-2^{99ile}, 54.5. The enzyme stability data for NAT-2^{99ile} were fitted to a first-order exponential decay curve, and the half-life of the enzyme was estimated to be 4 hr. For NAT-1 and NAT-2^{99asn}, the activities showed little or no change for 18 and 30 hr, respectively, and then decayed to 50% of their initial values at 45 and 60 hr, respectively. The greater stability of the rapid allelic variant, relative to the slow allelic variant, is evident in Fig. 5. Addition of dithiothreitol (2 mM final concentration) did not restore the enzyme activity (data not shown).

The stabilities of NAT-2 activities in A and B6 liver cytosols were determined at 37° with PABA, which is a specific substrate for the NAT-2 enzymes, as shown in Fig. 1. Initial activities were 5.7 and 3.2 nmol/min/mg of protein for B6 and A, respectively. The decline of PABA NAT activity in A liver fit a first-order process, with an estimated half-life of 2 hr. The PABA NAT activity of B6 liver cytosol did not change for 12 hr and then declined to 50% of its initial activity by 30 hr (Fig. 6).

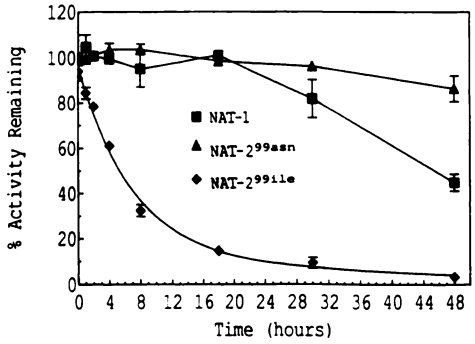

Fig. 5. Heat stability of NAT-1, NAT-2^{99asn}, and NAT-2^{99ile}. Cytosols from COS-1 cells acutely transfected with expression vectors encoding NAT-1, NAT-2^{99asn}, or NAT-2^{99ile} were incubated at 37° for the indicated periods of time and were assayed for NAT activity with 0.03 mM 2-AF and 0.5 mM AcCoA, as described in Materials and Methods. The activity is presented as percentage of initial activity, determined at time zero. Average values ± standard errors are shown for three experiments.

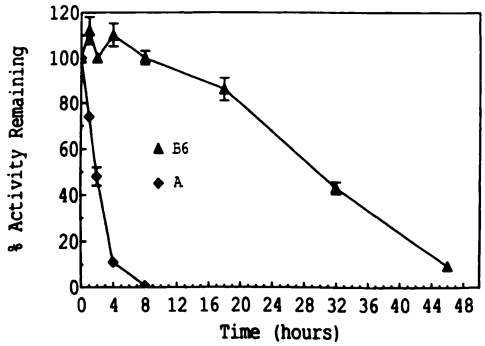

Fig. 6. Heat stability of PABA NAT activity of A and B6 liver cytosols. Cytosols from A and B6 mice were incubated at 37° for the indicated periods of time and were assayed for NAT activity with 0.1 mM PABA and 0.5 mM AcCoA, as described in Materials and Methods. The activity is presented as percentage of initial activity, determined at time zero. Average values ± standard errors are shown for three experiments.

The difference in heat stability between rapid and slow acetylator mouse liver cytosols is identical to the difference in stability observed between the rapid and slow allelic variants of NAT-2 in the transfected COS-1 cell cytosols.

Discussion

In the present study we have demonstrated that the intronless coding regions of the *Nat-1* and *Nat-2* genes expressed in COS-1 cells encode enzymes that catalyze *N*-acetylation of several different substrates. The substrate specificities of the transiently expressed enzymes agree well with *in vivo* and *in vitro* data reported previously. SMZ was shown not to be acetylated by hepatic cytosols from any of nine mouse strains tested (32), and later studies revealed that practically no hepatic SMZ-acetylating activity could be detected in 20 inbred mouse strains, including those studied earlier (7). In the current study, none of the cloned mouse enzymes was found to acetylate SMZ. PABA and 2-AF have been shown previously to be polymorphically acetylated by hepatic cytosols of B6 and A mice (7, 32) and, accordingly, in the transient expression system, NAT-2^{99asn}, the allele of NAT-2 from the rapid acetylator mouse strain (B6), had a significantly higher acetylating activity for PABA and 2-AF than did NAT-2^{99ile}, the corresponding allele of NAT-2 from the slow acetylator mouse strain (A). INH has been shown to be monomorphically acetylated in B6 and A mice *in vivo* (33). The current data support this observation, because INH was acetylated primarily by NAT-1 and only slightly and equivalently by NAT-2^{99asn} and NAT-2^{99ile}.

The activities determined for the cloned NAT-2 and NAT-1 indicate that they may correspond to the two distinct peaks of liver NAT activity separated by ion exchange fast protein liquid chromatography (34), because the substrate specificities of those two peaks conformed with those of the cloned enzymes. The association of cloned and expressed NAT-1 and NAT-2 with two distinct peaks of liver cytosol activity, on the basis of substrate preferences, has also been demonstrated for the human (9).

The substrate specificities of mouse NAT-1 and NAT-2 differ from those of human and rabbit NAT1 and NAT2. For example, mouse NAT-1 does not acetylate PABA, whereas both NAT-2^{99asn} and NAT-2^{99ile} acetylate PABA. Conversely, human and rabbit NAT1 catalyze acetylation of PABA (9, 20), but human NAT2 does not (9), and rabbit NAT2 has only a slight ability to acetylate PABA (20). SMZ is a preferred substrate for human and rabbit NAT2 and is acetylated by NAT1 of both species, but at a relatively slow rate (9, 20). However, SMZ is not acetylated by either of the mouse NATs. INH was preferentially acetylated by the mouse NAT-1 and poorly acetylated by NAT-2^{99asn} and NAT-2^{99ile}. INH acetylation by the cloned human or rabbit NAT1 and NAT2 has not yet been reported, although earlier studies in humans and rabbits indicate that INH is polymorphically acetylated in these species (35, 36). Of the substrates tested, 2-AF is the only one that is acetylated well by both enzymes in mice and humans (9). This relationship supports the use of the mouse as an animal model of the human acetylation polymorphism for arylamine carcinogenesis studies (37).

Comparison of the substrate specificities and deduced amino acid sequences of mouse NAT-2 and human NAT1 suggest that mouse NAT-2 and human NAT1 may be orthologous genes. Mouse NAT-2 has higher deduced amino acid identity with

human NAT1 (80%) than with human NAT2 (74%) (18). Nebert *et al.* (38) point out that assignment of orthologous genes across species according to their substrate specificities may be inaccurate, because orthologous genes may have differing catalytic activities. However, as additional information about conservation of the 5′-3′ orientation, of intron-exon structure, or of other features of the NAT gene structures among mammalian species becomes available, the assignment of orthologous genes may be possible.[1]

Kinetic constants determined from the expressed mouse NATs were comparable to those determined in mouse liver. Because PABA is acetylated exclusively by NAT-2, comparisons can be made between the PABA NAT activity of cloned forms of NAT-2 expressed in COS-1 cells and the PABA NAT activity in tissues of rapid and slow acetylators. In A and B6 liver, the apparent K_m for PABA was previously reported as <33 μM at 0.1 mM AcCoA (39). These values are consistent with the apparent K_m values determined for NAT-2^{99asn} and NAT-2^{99ile}, which were 6.8 ± 1.9 and 5.3 ± 2.1 μM, respectively (Table 2), at 0.1 mM AcCoA. The V_{max} difference between rapid and slow liver cytosols was 1.9-fold (39) at 0.1 mM AcCoA, which is comparable to the 1.6-fold difference seen with the expressed NATs (Table 2).

Kinetic constants for 2-AF of expressed NAT-1, NAT-2^{99asn}, and NAT-2^{99ile} also can be compared with those of mouse liver cytosols. These comparisons are complex because 2-AF, unlike PABA, is a substrate for both NAT-1 and NAT-2 and because the relative contributions of NAT-1 and NAT-2 to the total 2-AF NAT activity of rapid and slow acetylator livers differ. Apparent K_m values determined in A mouse liver were <33 μM (39), and this agrees with the apparent K_m values obtained for NAT-2^{99ile} (26.8 ± 4.5 μM) (Table 1). However, apparent K_m values obtained for B6 liver (82 μM) (39) are higher than the estimated apparent K_m values in the expressed enzyme system (40.1 ± 7.3 μM) (Table 1). Also, V_{max} differences between rapid and slow acetylators were 3-fold in liver (39) with 0.1 mM AcCoA, whereas the difference in V_{max} between NAT-2^{99asn} and NAT-2^{99ile} was 2-fold (Table 1). Despite the potential influences of the complexities mentioned above, the K_m and V_{max} values with 2-AF for isoforms of NAT-1 and NAT-2 expressed in an heterologous system are quite similar to those observed in mouse liver cytosols.

The Northern blot analysis (Fig. 2) indicates that mRNAs for Nat-1 and Nat-2 were both present in livers of rapid and slow acetylator mice and that Nat-2 mRNA was more abundant than Nat-1 mRNA. There was no difference in the relative quantity of hepatic Nat-1 mRNA between rapid and slow acetylators, nor was there any difference in the amount of Nat-2 mRNA between rapid and slow acetylators, according to the Betascope radioactivity determination (Fig. 3). These results indicate that the point mutation in the slow form of *Nat-2* does not appreciably affect the steady state levels of message. This finding is consistent with the observation that diverse point mutations responsible for the polymorphic forms of human NAT2 do not affect mRNA levels in slow acetylator humans (10), although another allelic variant, gene 3 (12), may be associated with attenuated mRNA levels.

There is a significant (approximately 15-fold) difference in the stability at 37° of the expressed rapid and slow allelic variants of NAT-2, judging from the times required for decline of NAT activity to 50% of the initial value. The same difference in stability was observed in liver cytosols. These findings suggest that differential stability of NAT-2 may contribute to mouse acetylation polymorphism. In humans, enzyme stability differences have been reported to contribute to slow acetylation in the case of the M2 NAT2 variant (10). The stabilities of human wild-type and M1-derived activities at 37° were identical (22 hr), whereas that of M2 was 6 hr.

It is interesting to speculate further about the molecular basis of acetylation polymorphism in B6 and A mice, in light of the observations we report. Expressed NAT-1 has no detectable specificity for PABA and, hence, would not be expected to contribute appreciably to the PABA-acetylating activity of cells. In contrast, both isoforms of NAT-2, NAT-2^{99asn} and NAT-2^{99ile}, possess specificity for PABA and their K_m values are equal or nearly equal. They should, therefore, contribute approximately equally to PABA NAT activity, if present in equal amounts. The mRNAs of both isoforms are produced in liver, as Northern blot analysis of B6 and A liver indicates, but, overall, the efficiency of the *Nat-2* gene of B6 appears to be greater (about 2-fold) than that of the *Nat-2* gene of A in translating its message into product, as shown by the *in vitro* translation experiment (Fig. 4). Finally, the expressed form of NAT-2^{99asn} is about 15 times more stable than that of NAT-2^{99ile}. Assuming that these effects occur independently in cells, one might expect the PABA-acetylating activity to be 15–30 times greater in tissues of rapid, compared with slow, acetylator mice [(0 activity with NAT-1) + 1 (no difference in K_m) × 1–2 (translational efficiency difference) × 15 (heat stability difference)].

The actual difference in PABA NAT activity in cytosols of B6 and A mouse livers, assayed under identical conditions, or the difference expressed as V_{max} values usually averages much less, about 2–3-fold (range, up to 8-fold) (39). The level of PABA NAT activity in mouse red blood cells, which lack protein-synthesizing machinery and in which NAT that is degraded is not replenished,[2] is 10–20-fold greater in B6 than in A mice (39), and this approaches the predicted value.

We have identified two specific factors, heat stability and translational efficiency of NAT-2, that may contribute to differences in the level of NAT activity in mouse liver. Further investigation should advance our understanding of the relative roles of these factors in regulating NAT activity in liver and other tissues of rapid and slow acetylator mice.

Acknowledgments

We thank Timothy P. Angelotti for his valuable assistance.

References

1. Weber, W. W., and S. N. Cohen. *N*-Acetylation of drugs: isolation and properties of *N*-acetyltransferase from rabbit liver. *Mol. Pharmacol.* **3**:266–273 (1967).
2. Weber, W. W. *The Acetylator Genes and Drug Response*. Oxford University Press, New York (1987).
3. Hearse, D. J., and W. W. Weber. Multiple *N*-acetyltransferases and drug metabolism. *Biochem. J.* **132**:519–526 (1973).
4. Hein, D. W., J. G. Omichinski, J. A. Brewer, and W. W. Weber. A unique pharmacogenetic expression of the *N*-acetylation polymorphism in the inbred hamster. *J. Pharmacol. Exp. Ther.* **220**:8–15 (1982).
5. Hein, D. W., T. D. Rustan, K. D. Bucher, E. J. Furman, and W. J. Martin. Extrahepatic expression of the *N*-acetylation polymorphism toward arylamine carcinogens in tumor target organs of an inbred rat model. *J. Pharmacol. Exp. Ther.* **258**:232–236 (1991).

[1] D. W. Nebert, personal communication.

[2] M. Wishnick and W. W. Weber, unpublished observations.

6. Glowinski, I. B., and W. W. Weber. Biochemical characterization of genetically variant aromatic amine *N*-acetyltransferases in A/J and C57BL/6J mice. *J. Biol. Chem.* **257**:1431–1437 (1982).
7. Glowinski, I. B., and W. W. Weber. Genetic regulation of aromatic amine *N*-acetylation in inbred mice. *J. Biol. Chem.* **257**:1424–1430 (1982).
8. Blum, M., D. M. Grant, W. McBride, M. Heim, and U. A. Meyer. Human arylamine *N*-acetyltransferase genes: isolation, chromosomal localization, and functional expression. *DNA Cell Biol.* **9**:193–203 (1990).
9. Grant, D. M., M. Blum, M. Beer, and U. A. Meyer. Monomorphic and polymorphic human arylamine *N*-acetyltransferases: a comparison of liver isozymes and expressed products of two cloned genes. *Mol. Pharmacol.* **39**:184–191 (1991).
10. Blum, M., A. Demierre, D. M. Grant, M. Heim, and U. A. Meyer. Molecular mechanism of slow acetylation of drugs and carcinogens in humans. *Proc. Natl. Acad. Sci. USA* **88**:5237–5241 (1991).
11. Ohsako, S., and T. Deguchi. Cloning and expression of cDNAs for polymorphic and monomorphic arylamine *N*-acetyltransferases from human liver. *J. Biol. Chem.* **265**:4630–4634 (1990).
12. Deguchi, T., M. Mashimo, and T. Suzuki. Correlation between acetylator phenotypes and genotypes of polymorphic arylamine *N*-acetyltransferase in human liver. *J. Biol. Chem.* **265**:12757–12760 (1990).
13. Vatsis, K. P., K. J. Martell, and W. W. Weber. Diverse point mutations in the human gene for polymorphic *N*-acetyltransferase. *Proc. Natl. Acad. Sci. USA* **88**:6333–6337 (1991).
14. Blum, M., D. M. Grant, A. Demierre, and U. A. Meyer. *N*-Acetylation pharmacogenetics: a gene deletion causes absence of arylamine *N*-acetyltransferase in liver of slow acetylator rabbits. *Proc. Natl. Acad. Sci. USA* **86**:9554–9557 (1989).
15. Sasaki, Y., S. Ohsako, and T. Deguchi. Molecular and genetic analyses of arylamine *N*-acetyltransferase polymorphism of rabbit liver. *J. Biol. Chem.* **266**:13243–13250 (1991).
16. Ozawa, S., Y. Abu-Zeid, Y. Kawakubo, S. Toyama, Y. Yamazoe, and R. Kato. Monomorphic and polymorphic isozymes of arylamine *N*-acetyltransferases in hamster liver: purification of the isozymes and genetic basis of *N*-acetylation polymorphism. *Carcinogenesis (Lond.)* **11**:2137–2144 (1990).
17. Abu-Zeid, M., K. Nagata, M. Miyata, S. Ozawa, M. Fukuhara, Y. Yamazoe, and R. Kato. An arylamine acetyltransferase (AT-I) from Syrian golden hamster liver: cloning, complete nucleotide sequence, and expression in mammalian cells. *Mol. Carcinogenesis* **4**:81–88 (1991).
18. Martell, K. J., K. P. Vatsis, and W. W. Weber. Molecular genetic basis of rapid and slow acetylation in mice. *Mol. Pharmacol.* **40**:218–227 (1991).
19. Jenne, J. W., F. M. MacDonald, and E. Mendoza. A study of the renal clearance, metabolic inactivation rates, and serum fall-off interaction of isoniazid and *para*-aminosalicylic acid in man. *Am. Rev. Respir. Dis.* **84**:371–378 (1961).
20. Blum, M., D. M. Grant, C. Saner, A. Demierre, M. Heim, D. D'Orazio, and U. A. Meyer. Rabbit acetylation polymorphism: molecular mechanism, in *Proceedings of the VIIIth International Symposium on Microsomes and Drug Oxidations* (M. Ingelman-Sundberg, J. A. Gustafsson, and S. Orrenius, eds.). Karolinska Institute, Stockholm, 39 (1990).
21. Huggenvik, J. I., M. W. Collard, R. E. Stofko, A. F. Seasholtz, and M. D. Uhler. Regulation of the human enkephalin promoter by two isoforms of the catalytic subunit of cyclic adenosine 3′,5′-monophosphate-dependent protein kinase. *Mol. Endocrinol.* **5**:921–930 (1991).
22. Chen, C., and H. Okayama. High-efficiency transformation of mammalian cells by plasmid DNA. *Mol. Cell. Biol.* **7**:2745–2752 (1987).
23. Andres, H. H., A. J. Klem, S. M. Szabo, and W. W. Weber. New spectrophotometric and radiochemical assays for acetyl-CoA:arylamine *N*-acetyltransferase applicable to a variety of arylamines. *Anal. Biochem.* **145**:367–375 (1985).
24. Kawakubo, Y., S. Manabe, Y. Yamazoe, T. Nishikawa, and R. Kato. Properties of cutaneous acetyltransferase catalyzing *N*- and *O*-acetylation of carcinogenic arylamines and *N*-hydroxyarylamine. *Biochem. Pharmacol.* **37**:265–270 (1988).
25. Herbommel, P., B. Bourachot, and M. Yaniv. Two distinct enhancers with different cell specificities coexist in the regulatory region of polyoma. *Cell* **39**:653–662 (1984).
26. Edlund, T., M. D. Walker, P. J. Barr, and W. J. Rutter. Cell-specific expression of the rat insulin gene: evidence for role of two distinct 5′ flanking elements. *Science (Washington D. C.)* **230**:912–916 (1985).
27. Gorman, C. High efficiency gene transfer into mammalian cells, in *DNA Cloning* (D. M. Glover, ed.). IRL Press, Oxford, UK, 143–165 (1986).
28. Cleland, W. W. The statistical analysis of enzyme kinetic data. *Adv. Enzymol.* **29**:1–32 (1967).
29. Weber, W. W. *N*-Acetyltransferase (mammalian liver), in *Metabolism of Amino Acids and Amines* (H. Tabor and C. W. Tabor, eds.). Academic Press, New York, 805–811 (1971).
30. Mattano, S. S., S. Land, C. M. King, and W. W. Weber. Purification and biochemical characterization of hepatic arylamine *N*-acetyltransferase from rapid and slow acetylator mice: identity with arylhydroxamic acid *N,O*-acyltransferase and *N*-hydroxyarylamine *O*-acetyltransferase. *Mol. Pharmacol.* **35**:599–609 (1989).
31. Chou, P. Y., and G. D. Fasman. Predictions of the secondary structure of proteins from their amino acid sequence. *Adv. Enzymol.* **47**:45–147 (1978).
32. Tannen, R. H., and W. W. Weber. Rodent models of the human isoniazid-acetylator polymorphism. *Drug Metab. Dispos.* **7**:274–279 (1979).
33. Tannen, R. H., and W. W. Weber. Antinuclear antibodies related to acetylator phenotype in mice. *J. Pharmacol. Exp. Ther.* **213**:485–490 (1980).
34. Hein, D. W., A. Trinidad, T. Yerokun, R. J. Ferguson, W. G. Kirlin, and W. W. Weber. Genetic control of acetyl coenzyme A-dependent arylamine *N*-acetyltransferase, hydrazine *N*-acetyltransferase, and *N*-hydroxy-arylamine *O*-acetyltransferase enzymes in C57BL/6J, A/J, AC57F1, and the rapid and slow acetylator A.B6 and B6.A congenic inbred mouse. *Drug Metab. Dispos.* **16**:341–347 (1988).
35. Weber, W. W. and D. W. Hein. Clinical pharmacokinetics of isoniazid. *Clin. Pharmacokinet.* **4**:401–422 (1979).
36. Weber, W. W., J. N. Miceli, D. J. Hearse, and G. S. Drummond. *N*-Acetylation of drugs: pharmacogenetic studies in rabbits selected for their acetylator characteristics. *Drug Metab. Dispos.* **4**:94–101 (1976).
37. Weber, W. W., S. S. Mattano, and G. N. Levy. Acetylation pharmacogenetics: acetylator phenotype and assessing susceptibility to aromatic amine carcinogens, in *Banbury Report 31: Carcinogen Risk Assessment: New Directions in the Qualitative and Quantitative Aspects of Carcinogen Risk Assessment* (R. Hart and F. D. Hoereger, eds.). Cold Spring Harbor Laboratory, New York, 81–92 (1988).
38. Nebert, D. W., D. R. Nelson, M. J. Coon, R. W. Estabrook, R. Feyereisen, Y. Fujii-Kuriyama, F. J. Gonzalez, F. P. Guengerich, I. C. Gunsalus, E. F. Johnson, J. C. Loper, R. Sato, M. R. Waterman, and D. J. Waxman. The P450 superfamily: update on new sequences, gene mapping, and recommended nomenclature. *DNA Cell Biol.* **10**:1–14 (1991).
39. Mattano, S. S., and W. W. Weber. Kinetics of arylamine *N*-acetyltransferase in tissues from rapid and slow acetylator mice. *Carcinogenesis* (Lond.) **8**:133–137 (1987).

Send reprint requests to: Dr. Wendell W. Weber, Department of Pharmacology, 6322 Medical Science Building 1, University of Michigan, Ann Arbor, MI 48109–0626.